

## POLYMORPHIC CRYSTALLIZATION OF AMINO ACID GLYCINE

Đến toà soạn 28-07-2024

**Khuu Chau Quang<sup>1,2,3</sup>, Le Dinh Phi<sup>1</sup>, Dang Chi Hien<sup>2,4</sup>,**  
**Trinh Thi Thanh Huyen<sup>1\*</sup>, Nguyen Anh Tuan<sup>1,2,4\*</sup>, Luu Cam Loc<sup>2,4</sup>**

<sup>1</sup>*Vietnamese-German University, VGU*

<sup>2</sup>*Graduated University of Science and Technology, VAST*

<sup>3</sup>*Industrial University of Ho Chi Minh City, IUH*

<sup>4</sup>*Institute of Chemical Technology, VAST,*

\*E-mail: huyen.ttt@vgu.edu.vn, natuan.ict.vast.vn@gmail.com

### TÓM TẮT

#### KẾT TỊNH ĐA CẤU TRÚC TỊNH THỂ AXIT AMIN GLYCINE

Nghiên cứu kết tinh chọn lọc cấu trúc tinh thể amino acid glycine chất lượng cao đạt chuẩn được diễn của Mỹ (FDA) và Châu Âu (EMA) là việc làm cần thiết trong ngành công nghiệp được trước khi được thương mại hóa trên thị trường thế giới. Trong nghiên cứu này, tinh thể glycine có ba dạng cấu trúc tinh thể khác nhau gồm  $\alpha$ -glycine,  $\beta$ -glycine và  $\gamma$ -glycine có thể được hình thành đồng thời trong quá trình kết tinh. Các cấu trúc tinh thể này có độ hòa tan khác nhau nên có hoạt tính sinh học và công thức thuốc khác nhau. Kiểm soát quá trình kết tinh các tinh thể đa cấu trúc rất phức tạp khi phụ thuộc vào nhiều yếu tố công nghệ. Do vậy, nghiên cứu kết tinh chọn lọc cấu trúc tinh thể mong muốn là việc làm đầy thử thách trong ngành công nghiệp dược. Kết quả nghiên cứu cho thấy 100% tinh thể  $\alpha$ -glycine được ưu tiên kết tinh tại chế độ thủy động lực 300 rpm, nồng độ ban đầu 300 g/L, tốc độ làm lạnh 5 °C/min, và nhiệt độ cuối của quá trình kết tinh 30 °C. Ngược lại hỗn hợp hai cấu trúc tinh thể  $\alpha$ -glycine và  $\gamma$ -glycine sẽ được ưu tiên kết tinh tại cùng nhiệt độ cuối 30 °C. Trong khi đó, hỗn hợp hai cấu trúc  $\alpha$ -glycine và  $\beta$ -glycine được kết tinh ở nhiệt độ cuối rất thấp khoảng -30 °C.

**Từ khoá:** đa cấu trúc tinh thể, mầm tinh thể, phát triển tinh thể, hình thái học tinh thể.

### 1. INTRODUCTION

Over 50% of organic and inorganic compounds can exist in different solid forms, which can be the amorphous (disordered state) or the crystalline (ordered state) [1-7]. Based on McCrone's definition, the polymorphism of any compound is its ability to crystallize as more than one distinct crystal species. Thus, the different molecular arrangements of the same chemical composition in a unit cell of crystal structure are called polymorphism. For pharmaceutical compounds, the term "polymorph/polymorphism" is used more

broadly by many authors and regulatory agencies, including the amorphous state, hydrate or solvate crystalline. The hydrate/solvate crystalline, sometimes called pseudo-polymorphs, where water/solvent molecules are incorporated in the crystal lattice stoichiometric or nonstoichiometric way. The solvate crystalline can also be known as a co-crystal, which consists of the active and solvent molecules in the unit cell of the crystal structure. In the pharmaceutical industry, the term "co-crystal" is understood broadly, where the two active molecules can be incorporated in the unit cell of the crystal structure in a solid

form. Due to different inter- and intramolecular interactions, including van der Waals and hydrogen bonding in crystal structures, the different polymorphs will have distinct free energies, leading to distinguish physical properties, such as solubility, bioactivity, chemical stability, melting point, and density, etc. Therefore, the polymorphism of a solid product in the crystallization process is considered a critical quality attribute [1-7]. The properties of solid products of any pharmaceutical companies will be evaluated, monitored, and licensed by the U.S. Food and Drug Administration (FDA) as well as the European Medicines Agency (EMA) to sell in the global market.

The global market size of amino acid glycine was valued at 5.0 billion USD in 2023, 5.3 billion USD in 2024, and grown to 8.3 billion USD by 2032, exhibiting an annual growth rate of 5.2% during the forecast period of 2024-2032. Thus, numerous previous studies have carried out glycine crystallization [8-13]. For example, a fast, continuous, non-seeded cooling crystallization of glycine in slug flow is studied to obtain a simple but reproducible process for generating uniform  $\alpha$ -glycine crystals with a narrow size distribution, which is always desired for both product quality and process efficiency purposes [8]. The laser-induced crystallization of glycine is also investigated under the Raman spectroscopy [9]. This study elucidates the complex interplay between optical forces, supersaturation, and crystallization dynamics to offer a new method for precisely controlling laser-induced crystallization. It is believed that the insights gained by this study pave the way for innovative developments in crystal chemistry and promising advancements in photochemistry [9]. For the crystallization

of glycine, a new method based on the ultrathin puddles created by gas blowing allows the formation of molecular layered crystals down to monolayer thickness on the surface [10]. This gas-blowing method opens up the opportunity to perform materials chemistry under confined conditions on the surface, allowing the formation of individual crystals of selected polymorphism [10]. Glycine has three crystal structures, including  $\alpha$ -form,  $\beta$ -form, and  $\gamma$ -form, in which  $\alpha$ -form and  $\beta$ -form are both unstable forms while  $\gamma$ -form is the most stable form [8,11]. At ambient conditions, the stability order of three polymorphs follows  $\beta$ -form< $\alpha$ -form< $\gamma$ -form [11]. Therefore, selective crystallization of glycine crystal structure is a challenging task in the pharmaceutical industry.

In contrast to previous studies, we developed a process for crystallizing glycine in a stirred tank. The stirred tank crystallizer is simple in design, easy to manufacture, and has low investment costs. It can be operated in both batch and continuous modes. In addition, it can be reused as other conventional stirred reactors. Thus, the nucleation and crystal growth mechanism must be understood to control the polymorphism in the stirred tank system. Accordingly, we focused on the intricate polymorphic glycine nucleation under different operating conditions. Here, the influence of the various fluid hydrodynamics, initial concentration, cooling rate, and final temperatures was investigated to reveal their role in determining the polymorphic glycine crystal product outcome.

## 2. EXPERIMENT

Glycine raw material (purity  $\geq$  98%) was purchased from Sigma-Aldrich Company without further purification. The standard batch stirred tank crystallizer consists of

Pyrex glass and has four baffles for adequate mixing [14-15]. The working volume of the crystallizer was 400 mL. The crystallization process to control the polymorphism of glycine was conducted using the cooling method. Glycine raw material was dissolved in the distilled water at a specific concentration and heated to 70 °C. Then, the cooling crystallization process was carried out to the final temperature of 30 °C and -30 °C. During the crystallization process, other factors included the agitation speed of 300 – 700 rpm, the cooling rate of 1 °C/min. – 5 °C/min., and the initial concentration of 200 - 400 g/L (see Figure 1).

The solute concentration was determined with utmost precision using UV-Vis spectroscopy (UV-Vis 1800 Shimadzu, Japan), which measures absorption at 205 nm. To define the polymorphic solubility, the raw material of glycine was added to 50 mL of distilled water and continuously stirred in a thermostatic bath at different temperatures. The solution sample was meticulously filtered with a 0.45 µm syringe filter to remove all fine crystals, then quickly diluted to prevent recrystallization when determining the saturation solubility at high temperatures.

The suspension in the crystallization process would be separated by vacuum filtration to gain the crystalline products and liquid phase. The crystalline products were washed with distilled water and dried in a desiccator over silica gel. The morphology of the crystalline product was observed and analyzed using an optical microscope (AmScope 40X-2500X), while the polymorphism was identified by X-ray diffraction (MAC Science, M18XHF-SRA). According to the time, the solute concentration in the liquid phase was defined and monitored via UV-Vis spectroscopy.

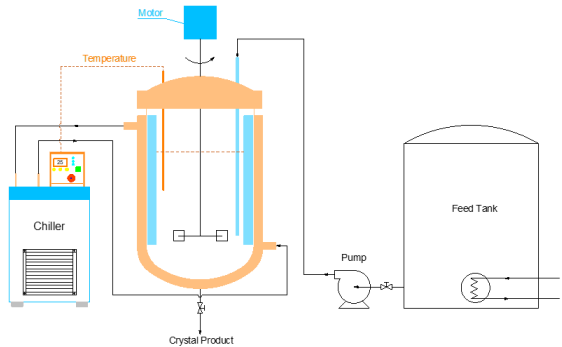


Figure 1. Schematic polymorphic crystallization process of glycine crystals

### 3. RESULTS AND DISCUSSION

The polymorphic glycine crystal morphology is distinguished, as shown in Figure 2a. Here, the  $\alpha$ -glycine and  $\beta$ -glycine have bipyramid-like and needle-like shapes, respectively (see Figure 2a (I)-(II)). Meanwhile, the  $\gamma$ -glycine owns the trigonal pyramid shape (see Figure 2a (III)). The unique morphology of these crystals is based on their distinct structures. The structure of  $\alpha$ -glycine belongs to the monoclinic system with space group  $P 21/n$ . The number of molecules in a unit cell is  $Z = 4$ , and the parameters of a unit cell are  $a = 5.0833 \text{ \AA}$ ,  $b = 11.902 \text{ \AA}$ , and  $c = 5.4399 \text{ \AA}$  with angles  $\alpha = 90^\circ$ ,  $\beta = 111.67^\circ$ , and  $\gamma = 90^\circ$ , as shown in Figure 2a (I). For  $\beta$ -glycine, the structure also belongs to the monoclinic system with space group  $P 21$ . However, the number of molecules in a unit cell is  $Z = 2$ , and the parameters of a unit cell are  $a = 5.311 \text{ \AA}$ ,  $b = 6.454 \text{ \AA}$ , and  $c = 5.694 \text{ \AA}$  with angles  $\alpha = 90^\circ$ ,  $\beta = 112.86^\circ$ , and  $\gamma = 90^\circ$ , as displayed in Figure 2a (II). In the case of  $\gamma$ -glycine, the structure belongs to the trigonal system with space group  $P 31$ . The number of molecules in a unit cell is  $Z = 3$ , and the parameters of a unit cell are  $a = 7.395 \text{ \AA}$ ,  $b = 7.395 \text{ \AA}$ , and  $c = 5.7 \text{ \AA}$  with angles  $\alpha = 90^\circ$ ,  $\beta = 90^\circ$ , and  $\gamma = 120^\circ$ , as depicted in Figure 2a (III).

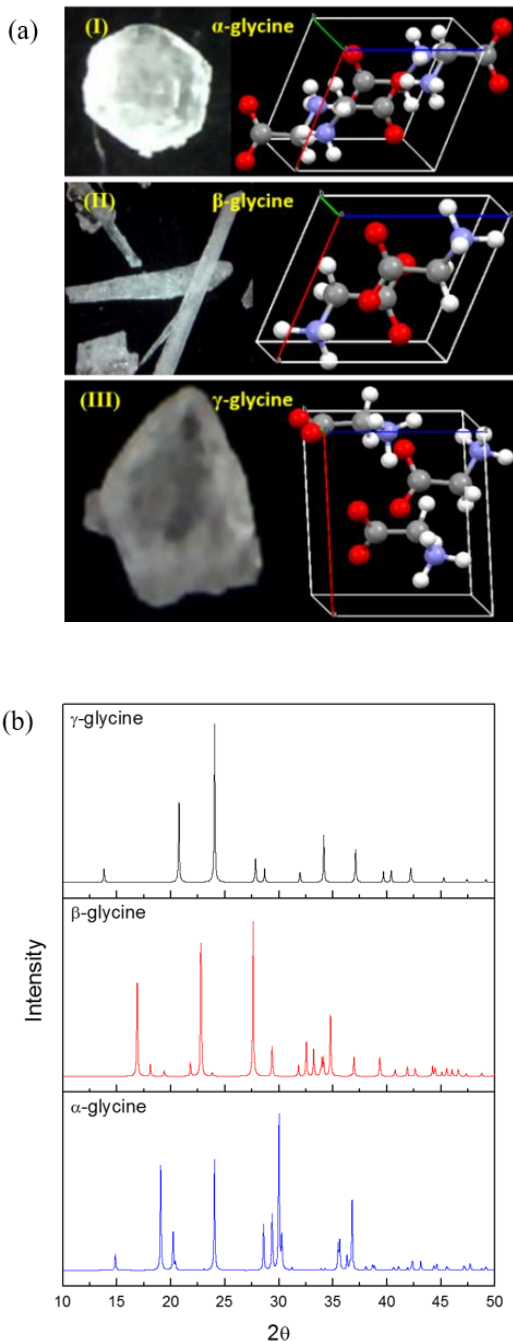


Figure 2. (a) Polymorphism of glycine crystals: (I)  $\alpha$ -glycine, (II)  $\beta$ -glycine, and (III)  $\gamma$ -glycine. (b) XRD pattern of polymorphic glycine crystals

The polymorphism of glycine could be confirmed via XRD spectroscopy, as shown in Figure 2b. The characteristic peaks of  $\alpha$ -glycine were  $2\theta \sim 14.65^\circ$ ,  $18.73^\circ$ ,  $19.91^\circ$ ,  $23.63^\circ$ ,  $29.67^\circ$ ,  $35.17^\circ$ ,  $40.60^\circ$ . Meanwhile, the distinctive peaks

of  $\beta$ -glycine would be  $2\theta \sim 18.05^\circ$ ,  $23.57^\circ$ ,  $28.59^\circ$ ,  $31.14^\circ$ ,  $33.67^\circ$ ,  $36.65^\circ$ ,  $39.13^\circ$ ,  $41.19^\circ$ ,  $53.20^\circ$ ,  $57.95^\circ$ . In the case of  $\gamma$ -glycine, the characteristic peaks were  $2\theta \sim 21.83^\circ$ ,  $25.30^\circ$ ,  $30.19^\circ$ ,  $33.64^\circ$ ,  $35.96^\circ$ ,  $39.08^\circ$ ,  $41.87^\circ$ ,  $44.47^\circ$ . Due to the different conformation and arrangement of molecules in the unit cell, the polymorphism of the solid products could be defined by the XRD method.

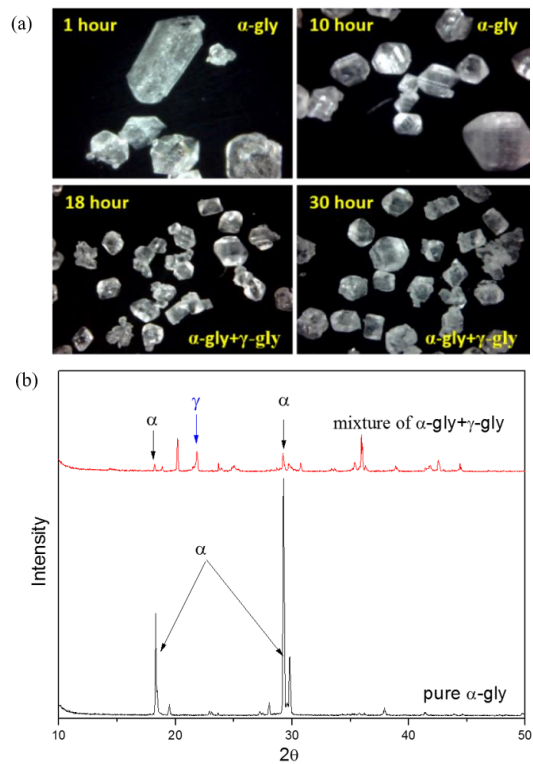


Figure 3. (a) Typical shape of  $\alpha$ -glycine and mixture of  $\alpha$ -glycine+ $\gamma$ -glycine according with the time; (b) XRD pattern of  $\alpha$ -glycine and mixture of  $\alpha$ -glycine+ $\gamma$ -glycine.

The crystallization was carried out using the cooling method from  $70^\circ\text{C}$  to the final crystallization temperature of  $30^\circ\text{C}$ . Here, the agitation speed was 300 rpm. Meanwhile, the initial concentration and cooling rate were 350 g/L and  $5^\circ\text{C}/\text{min}$ , respectively. We found that the initial crystals appeared in the  $\alpha$ -glycine form (see Figure 2a). After 10 hours, the crystals obtained were still in the  $\alpha$ -

glycine form. However, when the crystallization time was over 18 hours, a mixture of  $\alpha$ -glycine and  $\gamma$ -glycine crystals was obtained (see Figure 3a). That means a portion of the  $\alpha$ -glycine crystals had converted to the  $\gamma$ -glycine form by the Oswald ripening phase transition mechanism from a less stable crystal structure ( $\alpha$ -glycine) to a more stable crystal structure ( $\gamma$ -glycine) in the solution [5-6]. Over 24 hours (a day), the solid product obtained was still a mixture of the two forms of  $\alpha$ -glycine and  $\gamma$ -glycine. Thus, it implied that the phase transition time required to get 100%  $\gamma$ -glycine crystals might take several days or even a week.

The crystal structure of the solid product in Figure 3a was also confirmed by the characteristic peaks of the XRD spectroscopy in Figure 3b. The XRD spectrum in Figure 3b allowed us to conclude that 100% of the  $\alpha$ -glycine crystals would be crystallized before 18 hours from the start of the crystallization process, while a mixture of  $\alpha$ -glycine and  $\gamma$ -glycine crystal structures would be produced after 18 hours and last until 24 hours.

The hydrodynamic regime's effect on the polymorphic mapping is clearly shown in Figure 4a. Here, 100% of  $\alpha$ -glycine crystals would be crystallized and recovered within the first 18 hours at 300 rpm. However, when increasing the hydrodynamic regime to 700 rpm, the solid product obtained would be a mixture of  $\alpha$ -glycine and  $\gamma$ -glycine crystals within 5 hours (see Figure 4a). The time to recover 100%  $\alpha$ -glycine was only 4 hours at 700 rpm instead of 18 hours in the case of 300 rpm. Thus, to harvest the pure  $\alpha$ -glycine, the crystallization process should be operated at a low agitation speed.

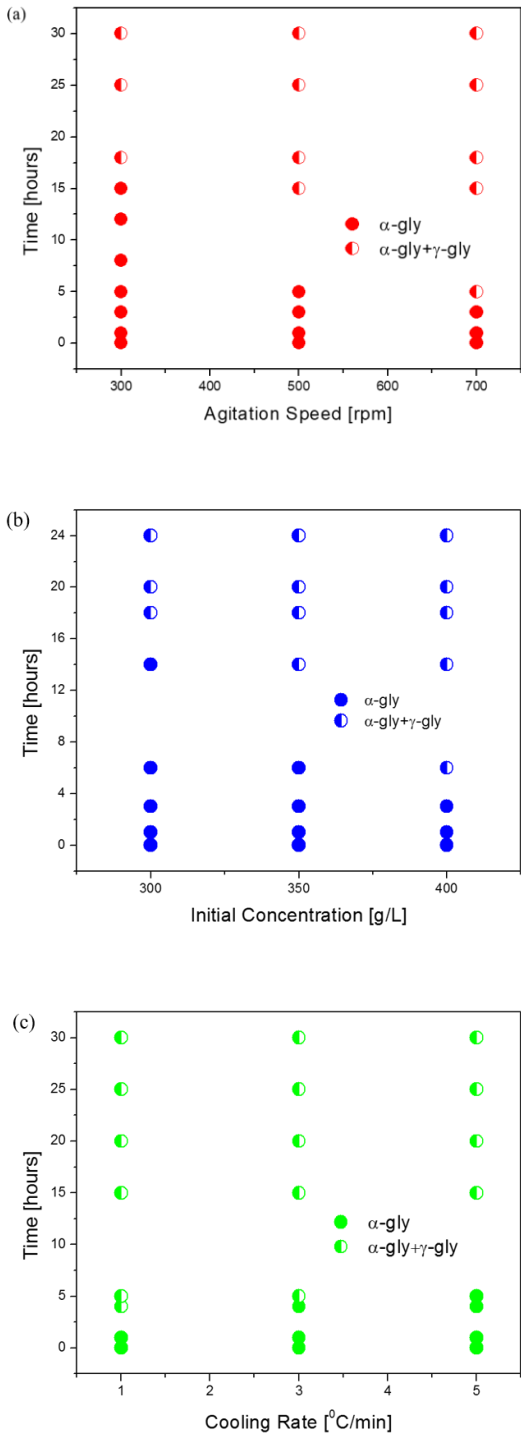


Figure 4. Polymorphic mapping of solid product varied with: (a) agitation speed and time at initial concentration of 350 g/L, and cooling rate of 5 °C/min.; (b) initial feed concentration with cooling rate of 5 °C/min., and (c) cooling rate with initial concentration of 350 g/L

The initial concentration's effect on the polymorphic mapping is summarized, as displayed in Figure 4b. At a low concentration of 300 g/L, the pure  $\alpha$ -glycine crystals were crystallized and recovered at 16 hours. However, when increasing the initial concentration to 400 g/L, the crystal product was a mixture of  $\alpha$ -glycine and  $\gamma$ -glycine at only 5 hours (see Figure 4b).

Thus, the time to recover the pure  $\alpha$ -glycine was about 4 hours at a high concentration of 400 g/L instead of 16 hours at a low concentration of 300 g/L. Accordingly, the pure  $\alpha$ -glycine could be controlled and harvested if we operated the crystallization process at a low initial concentration.

The cooling rate's effect on the polymorphic mapping of the solid product was also illustrated, as depicted in Figure 4c. At a high cooling rate of 5  $^{\circ}\text{C}/\text{min}$ ., the 100%  $\alpha$ -glycine crystals were precipitated at 14 hours. However, when reducing the cooling rate to 1  $^{\circ}\text{C}/\text{min}$ ., the solid product was a mixture of  $\alpha$ -glycine and  $\gamma$ -glycine at only 4 hours (see Figure 4c). Here, the crystallization time to obtain the 100%  $\alpha$ -glycine was only 4 hours at a low cooling rate of 1  $^{\circ}\text{C}/\text{min}$ . instead of 14 hours at a high cooling rate of 5  $^{\circ}\text{C}/\text{min}$ . Therefore, to harvest the pure  $\alpha$ -glycine, the crystallization process should be operated at a high cooling rate.

To study the formation of  $\beta$ -glycine crystals, we operated the crystallization process at the final temperature of -30  $^{\circ}\text{C}$  instead of the room temperature of 30  $^{\circ}\text{C}$ . In this condition, the solution concentration was 200 g/L, while the cooling rate and agitation speed were 5  $^{\circ}\text{C}/\text{min}$ . and 300 rpm, respectively. Here, we found that the  $\beta$ -glycine crystal appeared in the mixture of the  $\alpha$ -glycine and  $\beta$ -glycine forms (see Figure 5). Thus, it could be concluded that the  $\beta$ -glycine

nuclei were preferably precipitated at a low crystallization temperature of -30  $^{\circ}\text{C}$ . This result was confirmed by the XRD spectrum, where the characteristic peaks of the  $\beta$ -glycine crystal were observed, combining with that of the  $\alpha$ -glycine crystal (see Figure 5). Based on this result, it also referred that obtaining the pure  $\beta$ -glycine might take a long time, even several days, to have a completed phase transformation from the metastable  $\alpha$ -glycine form to the stable  $\beta$ -glycine form.

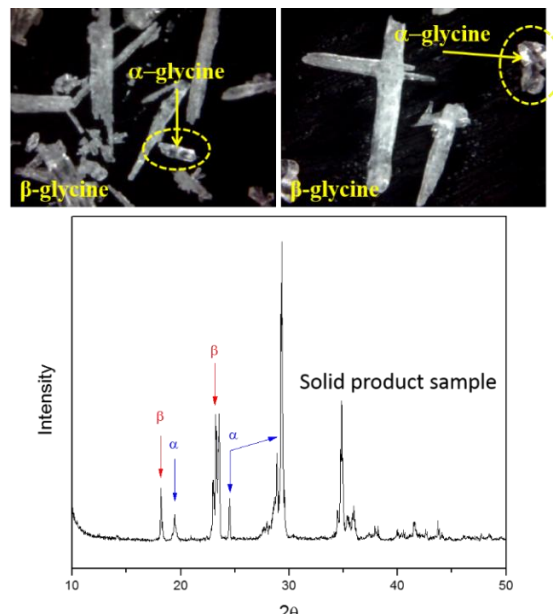


Figure 5. Crystal shape and structure of solid product at crystallization temperature of -30  $^{\circ}\text{C}$  at agitation speed of 300 rpm, and initial concentration of 300 g/L

#### 4. CONCLUSION

This study demonstrates the complexity of controlling the polymorphism during crystallization as it depends on varied technological parameters such as hydrodynamic regime, initial concentration, cooling rate, and final crystallization temperature. In the current work, we found that 100%  $\alpha$ -glycine crystals should be recovered at a low hydrodynamic regime of 300 rpm, low initial concentration of 300 g/L, high cooling rate of 5  $^{\circ}\text{C}/\text{min}$ ., and high final

temperature of 30 °C. Meanwhile, the  $\beta$ -glycine crystals should be crystallized at a low final temperature of -30 °C, and it might require a long time so that the  $\alpha$ -glycine structure can be completely converted to the desired  $\beta$ -glycine structure. In the case of  $\gamma$ -glycine crystals, we also found that this crystal should crystallize at high hydrodynamics above 700 rpm, high initial concentration of 400 g/L, low cooling rate of about 1 °C/min. and high final temperature of 30 °C. Similarly, to  $\beta$ -glycine, it might need a long time, sometimes up to several days, to completely transform from the unstable  $\alpha$ -glycine crystal to the stable  $\gamma$ -glycine crystal.

## REFERENCES

[1] Fellah N., Cruz I.J.C.D., Alamani B.G., Shtukenberg A.G., Pandit A.V., Ward M.D., Myerson A.S. (2024). Crystallization and Polymorphism under Nanoconfinement. *Crystal Growth & Design*, **24**, 3527-3558.

[2] Christopher L.B., Michael F.D., Baron G.P., Sarah L.P., Matteo S., Susan M.R.E., Louise S.P., Ravi K.R.A., Nicholas F., Vikram K., Yongsheng Z. (2024). Pharmaceutical Digital Design: From Chemical Structure through Crystal Polymorph to Conceptual Crystallization Process, *Crystal Growth & Design*, **24**, 5417-5438.

[3] Rolf H., Markus v.R. (2018). *Polymorphism in the Pharmaceutical Industry: Solid Form and Drug Development*, Weinheim: Wiley-VCH.

[4] Bernstein J. (2002). *Polymorphism in Molecular Crystals*, Oxford: Oxford University Press.

[5] Mullin J.W. (2001). *Crystallization*, Oxford: Butterworth-Heinemann.

[6] Myerson A.S., Deniz E., Alfred Y.L. (2019). *Handbook of Industrial Crystallization*, Cambridge: Cambridge University Press.

[7] Lee Y., Erdemir D., Myerson A.S. (2011). Crystal Polymorphism in Chemical Process Development, *Annu. Rev. Chem. Biomol. Eng.*, **2**, 259-280.

[8] Mou M., Jiang M. (2020). Fast Continuous Non-Seeded Cooling Crystallization of Glycine in Slug Flow: Pure  $\alpha$ -Form Crystals with Narrow Size Distribution, *J. Pharm. Innov.*, **15**, 281-294.

[9] Takahashi H., Yoshikawa H.Y., Sugiyama T. (2024). Raman spectroscopic study of concentration dynamics in glycine crystallization achieved by optical trapping. *Journal of Photochemistry & Photobiology, A: Chemistry*, **456**, 115845.

[10] Jincheng T., Nathan de B., Adriana A., Elizabeth J.L., Matthew B., Xiuju S., Alvin J.W., Andrew J.P., Michael W.A., Thomas V., Manuel M.F., Cinzia C. (2024). Crystallization of molecular layers produced under confinement onto a surface. *Nature Communications*, **15**, 1-8.

[11] Edward T.B., Hongyi X., Max T.B.C., Molly L., Fabio N., Xiaodong Z., Simon P. (2020). Polymorph evolution during crystal growth studied by 3D electron diffraction. *IUCrJ*, **7**, 5-9.

[12] Jingshan S.D., Yuna B., James J.D.Y. (2024). Non-classical crystallization in soft and organic materials, *Nature Reviews Materials*, **9**, 229-248.

[13] Hideki K., Tsubasa K., Rintaro H., Mitsuhiro K., Wahyudiono, Motonobu G. (2020). Ethanol-free antisolvent crystallization of glycine by liquefied dimethyl ether, *Heliyon*, **6**, e05258.

[14] Trinh Thi Thanh Huyen, Nguyen Thi Kim Phuong, Khuu Chau Quang, Wolf S.E., Nguyen Anh Tuan. (2022). Influence of Taylor Vortex Flow on the Crystallization of L-Glutamic Acid as an Organic Model Compound, *Ind. Eng. Chem. Res.*, **61**, 10205-10223.

[15] Thi Thanh Huyen Trinh, Chau Quang Khuu, Stephan E.W., Nguyen Anh Tuan. (2020). The multiple stages towards crystal formation of L-glutamic acid, *Journal of Crystal Growth*, **544**, 125727.